Mech. Sci., 8, 111–115, 2017
www.mech-sci.net/8/111/2017/
doi:10.5194/ms-8-111-2017

Mechanical Sciences
Open Access

A two-dimensional electron gas sensing motion of a nanomechanical cantilever

Andrey Shevyrin[1,2] **and Arthur Pogosov**[1,2]

[1]Rzhanov Institute of Semiconductor Physics SB RAS, Novosibirsk 630090, Russia
[2]Novosibirsk State University, Novosibirsk 630090, Russia

Correspondence to: Andrey Shevyrin (shevandrey@isp.nsc.ru)

Received: 1 November 2016 – Revised: 20 February 2017 – Accepted: 12 April 2017 – Published: 12 May 2017

Abstract. A quantitative physical model, describing the piezoelectric electromechanical coupling in nanomechanical resonators with a two-dimensional electron gas, is developed. Numerical calculations of the change in density of a two-dimensional electron gas contained in a vibrating cantilever are performed using the model and are shown to be consistent with the experiment. The obtained data show that the vibration-induced electron density modulation is localized near the clamping point and that it is related to a rapid spatial change in the mechanical stress near this point. It is shown that details of the clamping geometry significantly affect the magnitude of the effect.

1 Introduction

The low-dimensional electron systems, such as a two-dimensional electron gas (2DEG), quantum wires and quantum dots, have been intensively studied for decades, and these studies have led to discovery of bright phenomena including the integer (von Klitzing et al., 1980) and fractional (Goldman and Su, 1995) quantum Hall effects, weak localization (Altshuler et al., 1980), conductance quantization (van Wees et al., 1988), the Coulomb blockade (Meirav et al., 1990) etc. The usually studied low-dimensional electron systems are embedded in a semiconductor heterostructure being a part of a massive bulk. However, it is also possible to create micro- and nanomechanical resonators containing low-dimensional electron systems. Several papers report on non-trivial properties of hybrid GaAs / AlGaAs-based electromechanical systems combining the mechanical resonators and such mesoscopic devices as a single-electron transistor (Okazaki et al., 2016) and a quantum point contact (Cleland et al., 2002; Okazaki et al., 2013). Experiments (Tang et al., 2002; Shevyrin et al., 2015) show that the 2DEG conductivity is sensitive to vibrations of a resonator containing it, and it has been recently shown that this coupling is of piezoelectric origin (Shevyrin et al., 2016). However, there is still no common physical model describing the electromechanical coupling and predicting the magnitude of the effect. In the present paper, we propose a quantitative physical model that gives an opportunity to estimate the vibration-induced change in the electron density and reveals some important details of the electromechanical coupling in the nanoelectromechanical systems based on GaAs / AlGaAs heterostructures.

2 Model description

Consider a model nanoelectromechanical system representing a cantilever with a 2DEG (see Fig. 1a) similar to that experimentally studied in (Shevyrin et al., 2016). The cantilever, having thickness $t = 166$ nm, consists of the layers schematically shown in Fig. 1b. The 2DEG resides in the 13 nm-thick GaAs layer buried 77 nm below the surface. The cantilever studied in (Shevyrin et al., 2016) is created by means of selective etching of $Al_{0.8}Ga_{0.2}As$ sacrificial layer from under the top layers of the heterostructure. The etching front boundary forms the clamping. To avoid the stress singularity in our calculations, we consider a model system with a fillet of the radius R introduced in the corner between the remained sacrificial layer and the cantilever. Let the cantilever have length $L \gg t$ ($L = 3$ µm for the system studied in Shevyrin et al., 2016). We introduce a coordinate system with the x axis directed along the cantilever towards its free end and the y axis directed perpendicularly to the top surface

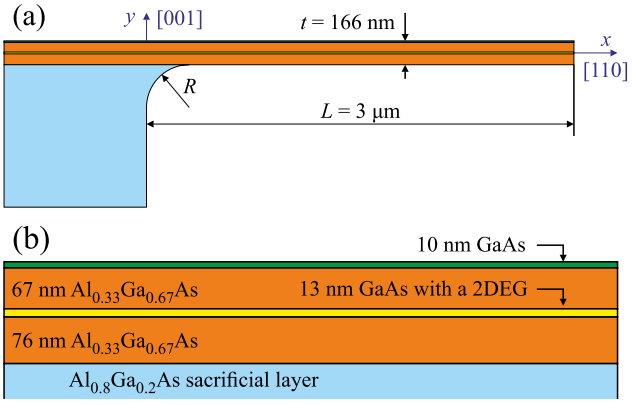

Figure 1. **(a)** Schematic image of the model cantilever and its orientation with respect to the crystallographic axes. L is the cantilever length, t is thickness, R is the fillet radius. **(b)** The heterostructure with a two-dimensional electron gas (2DEG) from which the model cantilever is created.

and pointing upwards. Let $x = 0$ at the vertical boundary of the remained sacrificial layer, and $y = 0$ at the middle plane of the cantilever. For simplicity, we restrict ourselves to the plane strain model assuming that displacements in the z direction are zero and no parameters are changed along this axis. Let the x axis coincide with piezoelectric-active [110] crystallographic direction and the y axis be directed along the [001] direction.

Let the cantilever perform flexural vibrations at the first eigenmode. The oscillating cantilever, being an electromechanical system, obeys the motion equation

$$\frac{\partial \sigma_{ij}}{\partial x_j} = -\rho \Omega_0^2 U_i \tag{1}$$

and the Gauss's law

$$\frac{\partial D_i}{\partial x_i} = 0. \tag{2}$$

Here σ_{ij} is stress tensor, ρ is mass density, Ω_0 is angular eigenfrequency, U_i is the displacement of a given point and D_i is electric displacement. The stress and the electric displacement can be expressed in terms of U_i and electric potential ϕ using the constitutive equations:

$$\sigma_{ij} = C_{ijkl}\frac{\partial U_k}{\partial x_l} + e_{kij}\frac{\partial \phi}{\partial x_k}, \tag{3}$$

$$D_i = e_{ijk}\frac{\partial U_j}{\partial x_k} - \epsilon\epsilon_0\frac{\partial \phi}{\partial x_i}, \tag{4}$$

where C_{ijkl} is stiffness tensor, e_{ijk} is piezoelectric tensor, ϵ is relative dielectric constant and ϵ_0 is the vacuum dielectric permittivity. Since tensors C_{ijkl} and e_{ijk} are symmetric, it is convinient to write them in the Voigt notations (Nye, 1985) as 6×6 and 6×3 matrices, respectively:

$$C_{ij} = \begin{pmatrix} \frac{C_{11}+C_{12}+2C_{44}}{2} & C_{12} & \frac{C_{11}+C_{12}-2C_{44}}{2} & 0 & 0 & 0 \\ C_{12} & C_{11} & C_{12} & 0 & 0 & 0 \\ \frac{C_{11}+C_{12}-2C_{44}}{2} & C_{12} & \frac{C_{11}+C_{12}+2C_{44}}{2} & 0 & 0 & 0 \\ 0 & 0 & 0 & C_{44} & 0 & 0 \\ 0 & 0 & 0 & 0 & \frac{C_{11}-C_{12}}{2} & 0 \\ 0 & 0 & 0 & 0 & 0 & C_{44} \end{pmatrix}, \tag{5}$$

$$e_{ij} = e_{14}\begin{pmatrix} 0 & 0 & 0 & 0 & 0 & 1 \\ 1/2 & 0 & -1/2 & 0 & 0 & 0 \\ 0 & 0 & 0 & -1 & 0 & 0 \end{pmatrix}. \tag{6}$$

Here $C_{11} = (11.88 + 0.14\chi) \times 10^{10}$ Pa, $C_{12} = (5.38 + 0.32\chi) \times 10^{10}$ Pa and $C_{44} = (5.94 - 0.05\chi) \times 10^{10}$ Pa are $Al_\chi Ga_{1-\chi}As$ elastic constants, and $e_{14} = -0.16 - 0.065\chi$ C m^{-2} is the piezoelectric constant (Adachi, 1985).

The substitution of Eqs. (3) and (4) in Eqs. (1) and (2) gives a system of partial differential equations. We solve this system using the finite element method on the full stack of the material shown in Fig. 1 and obtain eigenfrequency Ω_0, displacements U_i and potential ϕ. The vacuum surrounding the cantilever can be modeled as a media characterized by negligibly small stiffness, the zero piezoelectric tensor and dielectric constant $\epsilon = 1$. We apply Dirichlet conditions $U_i = 0$, $\phi = 0$ at the boundary that is far from the cantilever. A special area is the layer containing the 2DEG. When the cantilever bends, the 2DEG density changes in such a way as to maintain constant electrochemical potential. However, to simplify the calculations, we use the pure electrostatic screening model (Davies and Larkin, 1994) and consider the 2DEG as a media having a constant electrical potential. As shown in Shevyrin et al. (2016), this simplification is reasonable if the cantilever thickness far exceeds the Bohr radius $a_B = 4\pi\epsilon\epsilon_0\hbar^2 m^{-1} e^{-2} \approx 13$ nm (here m is an electron effective mass and e is the elementary charge). Thus, we neglect the chemical energy and model the 2DEG as a metal, or, equivalently, as a material with a dielectric constant far exceeding the constants of all other materials involved in the problem. Once the displacements U_x, U_y and the potential ϕ have been calculated, the electric displacement D_i can be found using Eq. (4), and the electron density change resulting from the cantilever bending can be found as $\delta n(x) = -e^{-1}(D_{y1} - D_{y2})$, where D_{y1} and D_{y2} are D_y values near the top and bottom 2DEG boundaries. The calculated electron density change, in the diffusive transport regime, should lead to a proportional change in the 2DEG conductivity $\delta\sigma = \delta n \times e\mu$, which can be measured experimentally (here μ is the electron mobility). Notice that, under the assumptions made, the calculated δn does not depend on the equilibrium electron density of a non-vibrating 2DEG.

3 Results and discussion

Figure 2a, b show the bending-induced changes in the electron density $\delta n(x)$ normalized to the deflection of the cantilever free end $U_y(L)$. The curves are calculated at the fillet

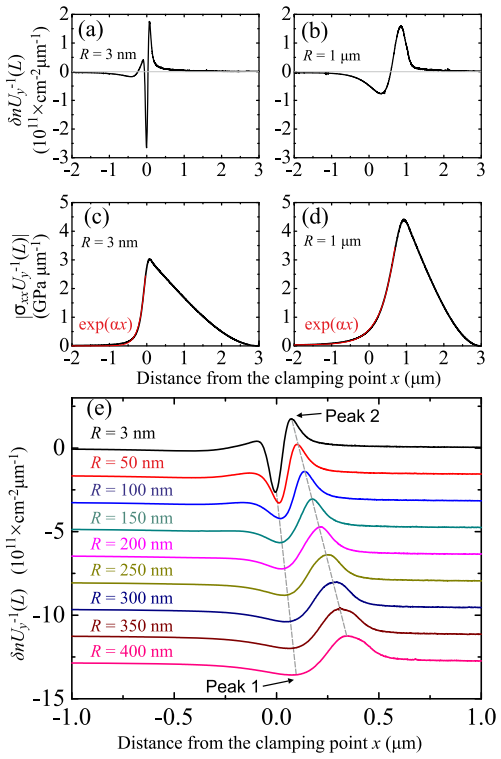

Figure 2. **(a, b)** The change in electron density $\delta n(x)$ normalized to deflection of the cantilever free end $U_y(L)$ calculated at the fillet radii $R = 3$ nm **(a)** and $R = 3$ μm **(b)**. **(c, d)** Corresponding mechanical stress σ_{xx} normalized to the free end deflection $U_y(L)$ calculated near the upper surface of the cantilever. Red lines show exponential fits to the data. **(e)** The change in electron density calculated at various fillet radii R (displayed in the figure). The curves are vertically offset by 1.6×10^{11} cm^{-2} μm^{-1} with respect to each other.

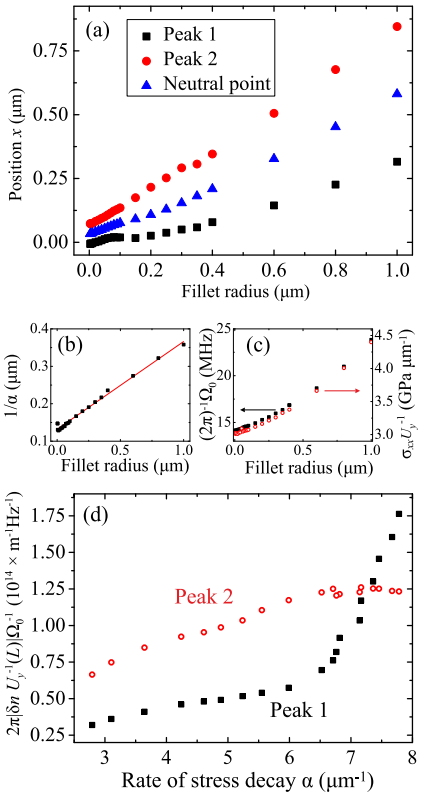

Figure 3. **(a)** Positions of the peaks in electron desnity change and the neutal point where the electron density change is zero. **(b)** The inverse rate of the stress decay α linearly depends on the fillet radius R. **(c)** The eigenfrequency f_0 and maximal mechanical stress σ_{xx} normalized to the free end deflection $U_y(L)$ as functions of the fillet radius. **(d)** Absolute amplitude of the peaks normalized to the free end deflection $U_y(L)$ and the eigenfrequency f_0 are determined by the stress decay rate α.

radii $R = 3$ nm (panel a) and $R = 1$ μm (panel b). Figure 2c, d show the corresponding absolute stress $|\sigma_{xx}U_y^{-1}(L)|$ calculated near the upper surface of the cantilever. It can be seen that the stress reaches its maximum near the clamping point and rapidly decreases to the left from the maximum. This stress drop can be roughly fitted by an exponent $|\sigma_{xx}U_y^{-1}(L)| = A\exp(\alpha x)$. The density change is most prominent near the maximal stress point. However, $\delta n(x)U_y^{-1}(L)$ decreases with increasing x much faster than the stress. Moreover, despite the maximal stess is higher at $R = 1$ μm, the density response is lower in this case than at $R = 3$ nm. This shows that the density change at a given point is not determined by the stress at this point. Instead, it is a functional of the spatial stress distribution and it is largely determined by the stress gradient near the considered point.

Figure 2e shows the $\delta n(x)U_y^{-1}(L)$ curves obtained at various fillet radii R. It can be seen that each of the obtained curves demonstrates two main peaks, one of which is negative (Peak 1) and the other is positive (Peak 2). At small R values, there is also a small region to the near left of Peak 1, where the electron density change is positive. This additional small peak is seemingly caused by the features associated to the stress concentration near the corner with a small curvature radius. It can be seen that, when R increases, the main peaks shift towards the free end of the cantilever, and the distance between them increases. Positions of the peaks and the neutral point, where $\delta n(x) = 0$, are shown in Fig. 3a as the functions of fillet radius R.

The change in fillet radius R leads to spatial redistribution of the stress. As shown in Fig. 3b, the increase in R leads to the increase in length α^{-1}, which is the distance characterizing the stress decay. Besides, it leads to the cantilever stiffening due to shortening of its effective length and increased thickness near the base. Figure 3c shows that this stiffening manifests itself in a growth of the eigenfrequency $(2\pi)^{-1}\Omega_0$ and an increase in the maximal stress $\sigma_{\max}$ normalized to the deflection $U_y(L)$ of the cantilever free end. Functions $\Omega_0(R)$ and $\sigma_{\max}U_y^{-1}(L)$ are similar, because both of them are roughly proportional to the effective value of tL^{-2}, where t is the cantilever thickness and L is its length.

Figure 3d shows the absolutized vibration-induced changes in the electron density (deviations from a uniform equilibrium value charactersistic for a resting cantilever), corresponding to the main peaks observed in Fig. 2e as functions of the rate of stress decay α. To reveal the effect of the α change and to separate this effect from the cantilever stiffening, these peak values are normalized to $(2\pi)^{-1}\Omega_0 U_y(L)$, rather than to $U_y(L)$, as in Fig. 2e. It can be seen that the considered peak values are determined by the rate of the stress decay α, and they increase with the increasing α. The peak values grow relatively slowly at $\alpha < 6\,\mu\text{m}^{-1}$, while, at $\alpha > 6\,\mu\text{m}^{-1}$, Peak 1 starts growing much faster, and Peak 2 reaches its saturation. This featured value of α approximately equals to the inverse cantilever thickness $t = 166$ nm. One can see from Fig. 3b that the same α value corresponds to the fillet radius $R \approx t$ at which an additional peak appears at the $\delta n(x)U_y^{-1}(L)$ dependence (see Fig. 2e). We suppose that the features, observed at the fillet radius being less than the cantilever thickness, are related to the high stress and the high gradients of the stress appearing near the fillet with a small radius.

The calculation results can be compared to the experimental results reported in Shevyrin et al. (2016). The change in the electron density at the distance of 1.3 µm from the clamping point, estimated from the experimental data, is about $\delta n \approx 5 \times 10^8\,\text{cm}^{-2}\,\mu\text{m}^{-1}$. The calculated value of δn corresponding to this distance is about $3 \times 10^8\,\text{cm}^{-2}\,\mu\text{m}^{-1}$, and it weakly depends on R at small radii. Thus, the results obtained from the developed model are consistent with the experiment. Notice that, at the distance of 1.3 µm, the change in the electron density is far below the change near the clamping point, and it would be desirable to compare the results obtained from the developed model to the change in the electron density experimentaly measured in the vicinity of the clamping point. However, to our knowledge, there are currently no papers reporting on such experimental results. Notice that the discussed change in the electron density is proportional to piezoelectric constant e_{14} and, in principle, it could be increased more than two times for GaN-based heterostructures.

So far we have discussed a cantilever with a naked surface. However, the geometry of the mesoscopic devices, such as single-electron transistors and quantum point contacts, is often determined by metal gates partially covering the surface. Obviously, the presence of the metal affects electron density, and the gated systems should be considered separately. In the following, we limit ourselves to the consideration of a cantilever similar to the system considered above, but with its top surface entirely covered with a thin metal layer. It is clear that this should lead to the cantilever stiffening, but we deliberately exclude this side effect from consideration by tending the metal elastic constants to zero. Thus, at the stage of the problem formulation, the appearance of the metal leads only to the zeroing electrical potential at the top surface. Figure 4a, b show the calculated $\delta n(x)U_y^{-1}(L)$ dependence obtained at $R = 0.1$ µm for the case of a metalized cantilever

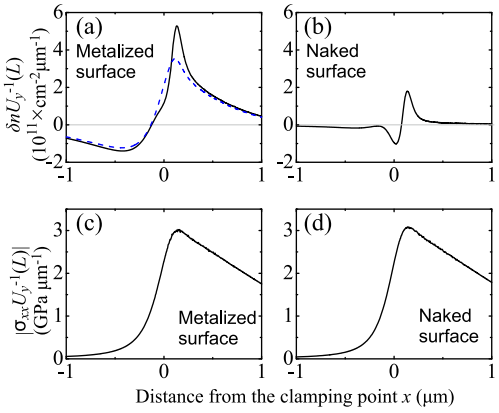

Figure 4. **(a, b)** Solid black lines: the change in electron density $\delta n(x)$ normalized to deflection of the cantilever free end $U_y(L)$ calculated for the cantilever covered with a metal **(a)** and cantilever with a naked surface **(b)**. The blue dashed line in **(a)** shows the difference between the signals in displayed in **(a, b)**. **(c, d)** Corresponding mechanical stress σ_{xx} normalized to $U_y(L)$ calculated near the top surface.

and for the case of a naked surface, respectively. Figure 4a shows also the difference of these two signals. Figure 4c, d show the corresponding spatial distributions of the stress. It can be seen that, in the case of a metalized cantilever, the electron density change consists of two components. One of them decreases with the increasing x as slowly as the stress, and the other (rapidly changing) is approximately equal to the density change observed in the case of a non-metalized cantilever. Notice that these two components have comparable magnitudes. Thus, the electron density change related to a rapid spatial change in the stress near the clamping point is significant even in the case of a metalized cantilever. In real mesoscopic devices, whose surface is only partially covered with metal, the density response is expected to be more complex and intermediary between the results of the two considered models.

4 Conclusions

The proposed physical model shows that the vibrations of a piezoelectric nanomechanical cantilever with a two-dimensional electron gas should lead to a change in the electron density. If the cantilever is not covered with a metal, such as a Schottky gate, then this change is prominent only near the clamping point and drops much faster than the stress with the increasing distance from this point. It is shown that the magnitude of the effect is determined mainly by the rate of the stress decay that occurs with the movement from the clamping point into the bulk, to which the cantilever is attached. It is demonstrated that the microscopic details of the clamping significantly affect the magnitude of the effect and should be taken into account. In the case of a cantilever cov-

ered with a metal, the considered localized change in the electron density is superimposed on a signal approximately proportional to the stress, but these components have comparable magnitudes.

Data availability. All datasets used in the manuscript can be requested from the corresponding author.

Competing interests. The authors declare that they have no conflict of interest.

Acknowledgements. The work is supported by the Russian Foundation for Basic Research grants 16-32-60130, 15-02-05774 and 16-02-00579. Part of this work related to the data interpretation was funded by the State Programme (grant No. 0306-2016-0015).

Edited by: M. K. Ghatkesar
Reviewed by: three anonymous referees

References

Adachi, S.: GaAs, AlAs and AlxGa1-xAs: Material parameters for use in research and device applications, J. Appl. Phys., 58, R1, doi:10.1063/1.336070, 1985.

Altshuler, B. L., Khmel'nitzkii, D., Larkin, A. I., and Lee, P. A.: Magnetoresistance and Hall effect in a disordered two-dimensional electron gas, Phys. Rev. B, 22, 5142, doi:10.1103/PhysRevB.25.2196, 1980.

Cleland, A. N., Aldridge, J. S., Driscoll, D. C., and Gossard, A. C.: Nanomechanical displacement sensing using a quantum point contact, Appl. Phys. Lett., 81, 1699, doi:10.1063/1.1497436, 2002.

Davies, J. H. and Larkin, I. A.: Theory of potential modulation in lateral surface superlattices, Phys. Rev. B, 49, 4800, doi:10.1103/PhysRevB.49.4800, 1994.

Goldman, V. J. and Su, B.: Resonant Tunneling in the Quantum Hall Regime: Measurement of Fractional Charge, Science, 267, 1010, doi:10.1126/science.267.5200.1010, 1995.

Meirav, U., Kastner, M. A., and Wind, S. J.: Charging and Periodic Conductance Resonances in GaAs Nanostructures, Phys. Rev. Lett., 65, 771, doi:10.1103/PhysRevLett.65.771, 1990.

Nye, J. F.: Physical Properties of Crystalls, London, Oxford University Press, 1985.

Okazaki, Y., Mahboob, I., Onomitsu, K., Sasaki, S., and Yamaguchi, H.: Quantum point contact displacement transducer for a mechanical resonator at sub-Kelvin temperatures, Appl. Phys. Lett., 103, 192105, doi:10.1063/1.4828890, 2013.

Okazaki, Y., Mahboob, I., Onomitsu, K., Sasaki, S., and Yamaguchi, H.: Gate-controlled electromechanical backaction induced by a quantum dot, Nat. Commun., 7, 11132, doi:10.1038/ncomms11132, 2016.

Shevyrin, A. A., Pogosov, A. G., Budantsev, M. V., Bakarov, A. K., Toropov, A. I., Rodyakina, E. E., and Shklyaev, A. A.: Actuation and transduction of resonant vibrations in GaAs/AlGaAs-based nanoelectromechanical systems containing two-dimensional electron gas, Appl. Phys. Lett., 106, 183110, doi:10.1063/1.4920932, 2015.

Shevyrin, A. A., Pogosov, A. G., Bakarov, A. K., and Shklyaev, A. A.: Piezoelectric Electromechanical Coupling in Nanomechanical Resonators with a Two-Dimensional Electron Gas, Phys. Rev. Lett., 117, 017702, doi:10.1103/PhysRevLett.117.017702, 2016.

Tang, H. X., Huang, X. M. H., Roukes, M. L., Bichler, M., and Wegscheider, W.: Two-dimensional electron-gas actuation and transduction for GaAs nanoelectromechanical systems, Appl. Phys. Lett., 81, 3879, doi:10.1063/1.1516237, 2002.

von Klitzing, K., Dorda, G., and Pepper, M.: New Method for High-Accuracy Determination of the Fine-Structure Constant Based on Quantized Hall Resistance, Phys. Rev. Lett., 45, 494, doi:10.1103/PhysRevLett.45.494, 1980.

van Wees, B. J., van Houten, H., Beenakker, C. W. J., Williamson, J. G., Kouwenhoven, L. P., van der Marel, D., and Foxon, C. T.: Quantized conductance of point contacts in a two-dimensional electron gas, Phys. Rev. Lett., 60, 848, doi:10.1103/PhysRevLett.60.848, 1988.